

# Spatial Structure of the $^{12}\text{C}$ Nucleus in a $3\alpha$ Model with Deep Potentials Containing Forbidden States

E. M. Tursunov,<sup>1,2,\*</sup> M. Z. Saidov,<sup>1,†</sup> and M. M. Begijonov<sup>1,‡</sup>

<sup>1</sup>*Institute of Nuclear Physics, Academy of Sciences,  
100214, Ulugbek, Tashkent, Uzbekistan*

<sup>2</sup>*National University of Uzbekistan, 100174, Tashkent, Uzbekistan*

The spatial structure of the lowest  $0_1^+$ ,  $0_2^+$ ,  $2_1^+$  and  $2_2^+$  states of the  $^{12}\text{C}$  nucleus is studied within the  $3\alpha$  model with the Buck, Friedrich and Wheatley  $\alpha\alpha$  potential with Pauli forbidden states in the  $S$  and  $D$  waves. The Pauli forbidden states in the three-body system are treated by the exact orthogonalization method. The largest contributions to the ground and excited  $2_1^+$  bound states energies come from the partial waves  $(\lambda, \ell) = (2, 2)$  and  $(\lambda, \ell) = (4, 4)$ . As was found earlier, these bound states are created by the critical eigen states of the three-body Pauli projector in the  $0^+$  and  $2^+$  functional spaces, respectively. These special eigen states of the Pauli projector are responsible for the quantum phase transitions from a weakly bound "gas-like" phase to a deep "quantum liquid" phase. In contrast to the bound states, for the Hoyle resonance  $0_2^+$  and its analog state  $2_2^+$ , dominant contributions come from the  $(\lambda, \ell) = (0, 0)$  and  $(\lambda, \ell) = (2, 2)$  configurations, respectively. The estimated probability density functions for the  $^{12}\text{C}(0_1^+)$  ground and  $2_1^+$  excited bound states show mostly a triangular structure, where the  $\alpha$  particles move at a distance of about 2.5 fm from each other. However, the spatial structure of the Hoyle resonance and its analog state have a strongly different structure, like  $^8\text{Be} + \alpha$ . In the Hoyle state the last  $\alpha$  particle moves far from the doublet at the distance between  $R = 3.0$  fm and  $R = 5.0$  fm. In the Hoyle analog  $2_2^+$  state the two alpha particles move at a distance of about 15 fm, but the last  $\alpha$  particle can move far from the doublet at the distance up to  $R = 30.0$  fm.

## I. INTRODUCTION

A discovery of quantum phase transition (QPT) in the  $\alpha$ -like nuclei [1], including  $^{12}\text{C}$  ground state, is one of the main phenomena in nuclear structure studies of last years. The effect was found within the framework of *ab initio* method based on the chiral effective field theory potentials. The importance of the finding is connected with a role of the carbon element in the Universe, thus allowing to conclude about "the life near a quantum phase transition" [1]. The *ab initio* method of [1] is of course a powerful tool for studying hyperfine effects from first principles of the quantum chromodynamics (QCD). In this sense the method has more predictive power than other approaches (see recent review [2] and references therein).

The discovery of the QPT in  $^{12}\text{C}$  inspired new research interest on the structure of this important quantum object. Very important question is, whether it is possible to observe an effect of the QPT within the framework of a  $3\alpha$ -cluster model for practical applications. Another interesting property of this nucleus is its special structure, associated with the Bose–Einstein condensation [3]. On the other hand a realistic modeling of Pauli forces in the  $3\alpha$  system is a very difficult problem. A complicated nonlocal  $\alpha\alpha$  potential derived from the resonating group model calculations was able to reproduce the energies of the ground state and the Hoyle ( $0_2^+$ ) resonance [4]. But a repulsive local  $\alpha\alpha$ -potentials, both  $l$ -dependent and  $l$ -independent, strongly underestimate the bound states of the  $^{12}\text{C}$  nucleus [5]. The alternative local deep  $\alpha\alpha$ - interaction potential of Buck–Friedrich–Wheatley (BFW) [6] yields much more realistic description of the nuclear structure, since it allows to treat the Pauli forbidden states (FS) exactly. However, application of the method of orthogonalizing pseudopotentials (OPP) [7] for the  $3\alpha$  quantum system met a serious problems, although it works very well for the structure of nuclei like  $^6\text{He}$  and  $^6\text{Li}$ , which contain a single  $\alpha$  cluster in the  $\alpha + N + N$  three-body model [8–12].

Indeed, detailed studies within the OPP method have demonstrated [13, 14] that the energy spectrum of the ground  $0_1^+$  and first excited  $2_1^+$  states is highly sensitive to the description of the  $\alpha\alpha$ -Pauli forbidden states. In these studies a convergence of the energies

---

\*Electronic address: tursune@inp.uz

†Electronic address: matlubsaidov7@gmail.com

‡Electronic address: marufjon19980310@gmail.com

of the ground and excited states in respect to the projecting constant  $\lambda$  was not clear. When passing values  $\lambda = 10^3$ – $10^4$  MeV the energies of the ground  $0_1^+$  and first excited  $2_1^+$  states increase sharply, which was not usual. Only the use of the direct orthogonalization method [13] for the elimination of the  $3\alpha$  Pauli forbidden states allowed to clarify the situation. It was found that the convergence problem within the OPP method is due to the so-called almost forbidden states (AFS) which are the special eigen states of the complete  $3\alpha$  Pauli projector with eigen values, close to zero.

Finally, recently in [15] it was argued that above AFS are nothing but the critical eigen states (CES) of the three-body Pauli projector which are responsible for the quantum phase transition in the ground and first excited  $2_1^+$  bound states of the  $^{12}\text{C}$  nucleus found in [1]. So, when passing the quantum critical eigen state, the energy of the lowest state of the carbon nucleus changes sharply from -0.627 MeV (weakly bound phase) to the deep phase with the energy value of -19.897 MeV. The same behavior was found for the excited  $^{12}\text{C}$  ( $2_1^+$ ) bound state where the weak phase with the energy of 1.873 MeV changes to the deep phase with the energy value of -16.572 MeV. Another interesting result is that from the left side of the quantum critical point the lowest states present the astrophysical significant Hoyle state  $0_2^+$  and its excited analog state  $2_2^+$ . When passing the above mentioned CES these Hoyle states energies almost do not change, but they become the excited states. In other words the lowest  $0_1^+$  and  $2_1^+$  states in the deep phases are created by the critical eigen states of the complete three-alpha Pauli projector.

The aim of the present work is to study the spatial structure of the ground and lowest excited states of the  $^{12}\text{C}$  nucleus in the  $3\alpha$  model. In [16] the spatial structure was studied within the local  $\alpha\alpha$  potentials with a strong repulsive core, while adding a very large three-body attractive forces. Differently, we deal with a more realistic deep BFW  $\alpha\alpha$  potential with forbidden states in the  $S$  and  $D$  waves. A variational method on symmetrized Gaussian basis is employed. For the elimination of the  $3\alpha$  Pauli forbidden states we use the same direct orthogonalization method from [13, 15]. We will examine a similarity of the  $0^+$  and  $2^+$  spatial structure including the Hoyle band.

The theoretical model is described in Section 2. Sections 3 contains the numerical results for the  $^{12}\text{C}(0^+)$  and  $^{12}\text{C}(2^+)$  states. Conclusions are given in the last section.

## II. THEORETICAL MODEL

The direct orthogonalization method [13, 15] is based on the separation of the complete Hilbert functional space into two parts. The first allowed subspace  $L_Q$  is defined by the kernel of the  $3\alpha$  projector. The rest subspace  $L_P$  contains  $3\alpha$  states forbidden by the Pauli principle. The complete Hilbert functional space of  $3\alpha$  states is separated into the  $L_Q$  (allowed) and  $L_P$ (forbidden) subspaces, then the three-body Schrödinger equation is solved in  $L_Q$ .

The  $\alpha\alpha$ - interaction potential of Buck–Friedrich–Wheatley [6] of the Gaussian form reads

$$V(r) = V_0 \exp(-\eta r^2) + 4e^2 \operatorname{erf}(br)/r, \quad (1)$$

with parameters  $V_0 = -122.6225$  MeV,  $\eta = 0.22$  fm<sup>-2</sup> for the nuclear part and  $b = 0.75$  fm<sup>-1</sup> for the Coulomb part. This choice of the potential parameters yields a very good description of the experimental phase shifts  $\delta_L(E)$  for the  $\alpha\alpha$ - elastic scattering in the partial waves  $L = 0, 2, 4$  within the energy range up to 40 MeV and the energy positions and widths of the <sup>8</sup>Be resonances.

As in [13, 15] we use a value  $\hbar^2/m_\alpha = 10.4465$  MeV fm<sup>2</sup>. This potential contains two Pauli forbidden states in the  $S$  wave with energies  $E_1 = -72.6257$  MeV and  $E_2 = -25.6186$  MeV, and a single forbidden state in the  $D$  wave with  $E_3 = -22.0005$  MeV. A realistic description of the system requires to eliminate all FS from the solution of the three-body Schrödinger equation.

The three-body Hamiltonian reads:

$$\hat{H} = \hat{H}_0 + V(r_{23}) + V(r_{31}) + V(r_{12}), \quad (2)$$

where  $\hat{H}_0$  is the kinetic energy operator and  $V(r_{ij})$  is the interaction potential between the  $i$ -th and  $j$ -th particles. A solution of the Schrödinger equation

$$\hat{H}\Psi_s^{JM} = E\Psi_s^{JM}, \quad \Psi_s^{JM} \in L_Q. \quad (3)$$

should belong to the allowed subspace  $L_Q$  of the complete  $3\alpha$  functional space.

The symmetrized wave function of the  $3\alpha$ - system is expanded in the series of Gaussian functions [14]:

$$\Psi_s^{JM} = \sum_{\gamma j} c_j^{(\lambda, l)} \varphi_{\gamma j}^s, \quad (4)$$

where  $\varphi_{\gamma j}^s = \varphi_{\gamma j}(1; 2, 3) + \varphi_{\gamma j}(2; 3, 1) + \varphi_{\gamma j}(3; 1, 2)$ ,

$$\varphi_{\gamma j}(k; l, m) = N_j^{(\lambda l)} x_k^\lambda y_k^l \exp(-\alpha_{\lambda j} x_k^2 - \beta_{l j} y_k^2) \mathcal{F}_{\lambda l}^{JM}(\widehat{\mathbf{x}}_{\mathbf{k}}, \widehat{\mathbf{y}}_{\mathbf{k}}) \quad (5)$$

Here  $(k; l, m) = (1; 2, 3), (2; 3, 1), (3; 1, 2)$ ,  $\gamma = (\lambda, l, J, M) = (\gamma_0, J, M)$ ;  $\mathbf{x}_{\mathbf{k}}, \mathbf{y}_{\mathbf{k}}$  are the normalized Jacobi coordinates in the  $k$ -set:

$$\begin{aligned} \mathbf{x}_{\mathbf{k}} &= \frac{\sqrt{\mu}}{\hbar} (\mathbf{r}_1 - \mathbf{r}_m) \equiv \tau^{-1} \mathbf{r}_{1,m}; \\ \mathbf{y}_{\mathbf{k}} &= \frac{2\sqrt{\mu}}{\sqrt{3}\hbar} \left( \frac{\mathbf{r}_1 + \mathbf{r}_m}{2} - \mathbf{r}_k \right) \equiv \tau_1^{-1} \rho_{\mathbf{k}}, \end{aligned} \quad (6)$$

$N_j^{(\lambda l)}$  is a normalizing multiplier. The nonlinear variational parameters  $\alpha_{\lambda j}, \beta_{l j}$  are chosen as the nodes of the Chebyshev grid:

$$\begin{aligned} \alpha_{\lambda j} &= \alpha_0 \tan\left(\frac{2j-1}{2N_\lambda} \frac{\pi}{2}\right), j = 1, 2, \dots, N_\lambda, \\ \beta_{l j} &= \beta_0 \tan\left(\frac{2j-1}{2N_l} \frac{\pi}{2}\right), j = 1, 2, \dots, N_l, \end{aligned} \quad (7)$$

where  $\alpha_0$  and  $\beta_0$  are scale parameters for each  $(\lambda l)$  partial component of the complete wave function.

When one uses the Chebyshev grid, the basis frequencies  $\alpha_{\lambda j}, \beta_{l j}$  cover larger and larger intervals around the scale parameters as the numbers  $N_\lambda$  and  $N_l$  increase. This allows to take into account both short-range and long-range correlations of particles. The extraordinary flexibility of the many-particle Gaussian basis makes it possible to describe three-particle configurations that are formed in the ground and excited states of multicluster systems, and which exhibit an extremely high degree of clustering [17].

The angular part of the Gaussian basis is factorized as:

$$\mathcal{F}_{\lambda l}^{JM}(\widehat{\mathbf{x}}_{\mathbf{k}}, \widehat{\mathbf{y}}_{\mathbf{k}}) = \{Y_\lambda(\widehat{\mathbf{x}}_{\mathbf{k}}) \otimes Y_l(\widehat{\mathbf{y}}_{\mathbf{k}})\}_{JM} \phi(1)\phi(2)\phi(3), \quad (8)$$

where  $\phi(i)$  is the internal wave functions of the  $\alpha$ -particles. Here the orbital momenta  $\lambda$  and  $l$  are conjugate to the Jacobi coordinates  $\mathbf{x}_{\mathbf{k}}$  and  $\mathbf{y}_{\mathbf{k}}$ , respectively.

The kinetic energy operator of the Hamiltonian can be expressed in the normalized Jacobi coordinates in a simple form as

$$\hat{H}_0 = -\frac{\partial^2}{\partial \mathbf{x}_{\mathbf{k}}^2} - \frac{\partial^2}{\partial \mathbf{y}_{\mathbf{k}}^2} \quad (9)$$

within any choice of  $(\mathbf{x}_{\mathbf{k}}, \mathbf{y}_{\mathbf{k}})$ ,  $k = 1, 2, 3$ . The detailed matrix elements of all the operators can be found in [17].

In order to separate the complete  $3\alpha$  functional space into the  $L_Q$  and  $L_P$  one has to calculate eigen states and corresponding eigen values of the operator [13]

$$\hat{P} = \sum_{i=1}^3 \hat{P}_i, \quad (10)$$

where each  $\hat{P}_i$ , ( $i = 1, 2, 3$ ) is the sum of Pauli projectors  $\hat{\Gamma}_i^{(f)}$  on the partial  $f$  wave forbidden states ( $1S$ ,  $2S$ , and  $1D$ ) in the  $i$ -th  $\alpha\alpha$  subsystem:

$$\hat{P}_i = \sum_f \hat{\Gamma}_i^{(f)}, \quad (11)$$

$$\hat{\Gamma}_i^{(f)} = \frac{1}{2f+1} \sum_{m_f} | \varphi_{fm_f}(\mathbf{x}_i) \rangle \langle \varphi_{fm_f}(\mathbf{x}'_i) | \delta(\mathbf{y}_i - \mathbf{y}'_i), \quad (12)$$

with the forbidden state function expanded into the Gaussian basis:

$$\varphi_{fm_f}(\mathbf{x}_i) = x_i^f \sum_m N_m^{(f)} b_m^{(f)} \exp\left(-\frac{r_i^2}{2r_{0m}^2}\right) Y_{fm_f}(\hat{\mathbf{x}}_i). \quad (13)$$

Here  $r_0$  is the "projector radius" and  $N_m^{(f)}$  is the normalizing multiplier:

$$N_m^{(f)} = 2^{f+7/4} \frac{\alpha_m^{(2f+3)/4}}{\pi^{1/4} [(2\lambda+1)!!]^{1/2}}, \quad \alpha_m = \tau^2 / (2r_{0m}^2). \quad (14)$$

The operator  $\hat{P}$  is not a complete projector for the three-body system, however its kernel is identical with the kernel of the complete three-body projector [18]. This is why one can use the operator  $\hat{P}$  for the separation of the complete Hilbert functional space into the allowed  $L_Q$  and forbidden  $L_P$  subspaces.

For the study of spatial structure of the  $^{12}\text{C}$  nucleus lowest states in the  $3\alpha$  model we have to estimate the probability density functions

$$P(r, R) = \int \Psi_s^{JM*}(\mathbf{r}, \mathbf{R}) \Psi_s^{JM}(\mathbf{r}, \mathbf{R}) d\hat{\mathbf{r}} d\hat{\mathbf{R}}, \quad (15)$$

for each of the fixed bound or resonance state. In the last equation the integral is taken only over angular part of the relative coordinates  $\mathbf{r}$  (distance between any fixed two  $\alpha$  particles) and  $\mathbf{R}$  (distance between the last  $\alpha$  and the center of mass of already fixed two  $\alpha$  particles).

The normalization of the spatial density function requires the condition

$$\int P(r, R) dr dR = 1. \quad (16)$$

TABLE I: Contributions of different partial waves in % into the  $0_1^+$  (ground) and  $0_2^+$  (Hoyle) states

$(\lambda, \ell)$	(0, 0)	(2, 2)	(4, 4)	(6, 6)	(8, 8)
$0_1^+$	28.777	35.722	34.885	0.606	0.010
$0_2^+$	55.012	24.120	17.008	3.418	0.442

TABLE II: Contributions of different partial waves in % into the  $2_1^+$  and  $2_2^+$  (Hoyle analog) states

$(\lambda, \ell)$	(0, 2)	(2, 0)	(2, 2)	(2, 4)	(4, 2)	(4, 4)	(6, 6)	(6, 4)	(4, 6)	(8, 8)	(8, 6)	(6, 8)
$2_1^+$	7.186	7.199	44.240	0.736	0.724	39.313	0.586	0.005	0.004	0.008	0	0
$2_2^+$	12.680	10.588	73.444	0.044	2.797	0.062	0.125	0.101	0.031	0.025	0.044	0.058

### III. NUMERICAL RESULTS

#### A. Partial Waves Contributions to the Lowest $0^+$ and $2^+$ States

First we estimate the contributions of different three-body partial waves into the energies of the ground and excited states of the  $^{12}\text{C}$  nucleus. For the  $0_1^+$  (ground) and  $0_2^+$  (Hoyle) states the main contributions come from the three-body channels  $(\lambda, \ell) = (0, 0), (2, 2), (4, 4)$  which contain up to 280 Gaussian functions. Convergence is fast due to the use of symmetrized basis functions. Alternatively, one can use a nonsymmetrized basis functions for practical applications of the three-body wave function. In this case the main contributions come from the three-body channels  $(\lambda, \ell) = (0, 0), (2, 2), (4, 4), (6, 6), (8, 8)$  requiring up to 1008 Gaussian functions for obtaining convergent results comparable with the results of the symmetrized basis.

In Table 1 we give the contributions of different partial waves into the  $0_1^+$  (ground) and  $0_2^+$  (Hoyle) states. The ground state energy in the deep phase is -19.90 MeV, which was obtained by including the quantum critical eigen state of the Pauli projector into the functional model space of the  $0^+$  states [15]. A big difference of this number from the experimental energy value of -7.275 MeV means that the  $3\alpha$  system can be in this deep phase with a probability much smaller than 1. Beyond the critical point the energy of the Hoyle state increases slightly to  $E = -0.458$  MeV, which is, however, lower than the experimental energy value  $E_{\text{exp}}(0_2^+) = 0.380$  MeV [15]. Then a small three-body potential is needed for the reproduction of the experimental energy.

As can be seen from the table, for the ground state the largest contributions come from the partial waves  $(\lambda, \ell) = (2, 2)$  and  $(\lambda, \ell) = (4, 4)$ . The contribution of the  $S$  wave is smaller due to the presence of Pauli forbidden states. In contrast to the ground state, the main contribution to the Hoyle state comes from  $S$  waves. This result supports an idea of a possible condensation of the  $\alpha$  particles in the Hoyle state [2].

For the  $2_1^+$  (bound) and  $2_2^+$  (Hoyle analog) states the most important contributions come from the three-body channels  $(\lambda, \ell) = (0, 2), (2, 0), (2, 2), (2, 4), (4, 2), (4, 4)$  which contain up to 437 symmetrized Gaussian functions. Or, alternatively, non-symmetrized basis functions can be used within the three-body channels  $(\lambda, \ell) = (0, 2), (2, 0), (2, 2), (2, 4), (4, 2), (4, 4), (4, 6), (6, 4), (6, 6), (6, 8), (8, 6), (8, 8)$ . In the last case a convergent results were obtained with 1292 Gaussian functions.

In Table 2 we give the contributions of different partial waves to the  $2_1^+$  (bound) and  $2_2^+$  (Hoyle analog) states. The energy of the  $2_1^+$  state in the deep phase is -16.572 MeV, which was obtained by including the quantum critical eigen state of the Pauli projector into the functional model space of the  $2^+$  states [15]. As in the case of the ground state, a strong difference of this number from the experimental energy value of -2.836 MeV means that the  $3\alpha$  system can be in this deep phase with a probability much smaller than 1. Beyond the critical point the energy of the Hoyle analog state increases slightly to  $E = 2.279$  MeV, which is close to the experimental energy value  $E_{\text{exp}}(2_2^+) = 2.596$  MeV [15]. The same small additional three-body potential, which was used for fitting Hoyle state energy, can reproduce the experimental energy of its analog state [15].

From Table 2 one can see that for the  $2_1^+$  state the largest contributions come from the partial waves  $(\lambda, \ell) = (2, 2)$  and  $(4, 4)$ . The contributions of the partial  $S$  waves  $(\lambda, \ell) = (0, 2)$  and  $(2, 0)$  are comparable and smaller due to the presence of Pauli forbidden states. For the  $2_2^+$  Hoyle analog state the dominant contribution comes from the partial wave  $(\lambda, \ell) = (2, 2)$ .

## B. Probability Density Functions of the Lowest $0^+$ and $2^+$ States

Now we go to estimate the probability density functions of the lowest  $0^+$  and  $2^+$  states of the carbon nucleus on the base of Eq. (15). These functions yield a spatial structure or a matter distribution in each state.



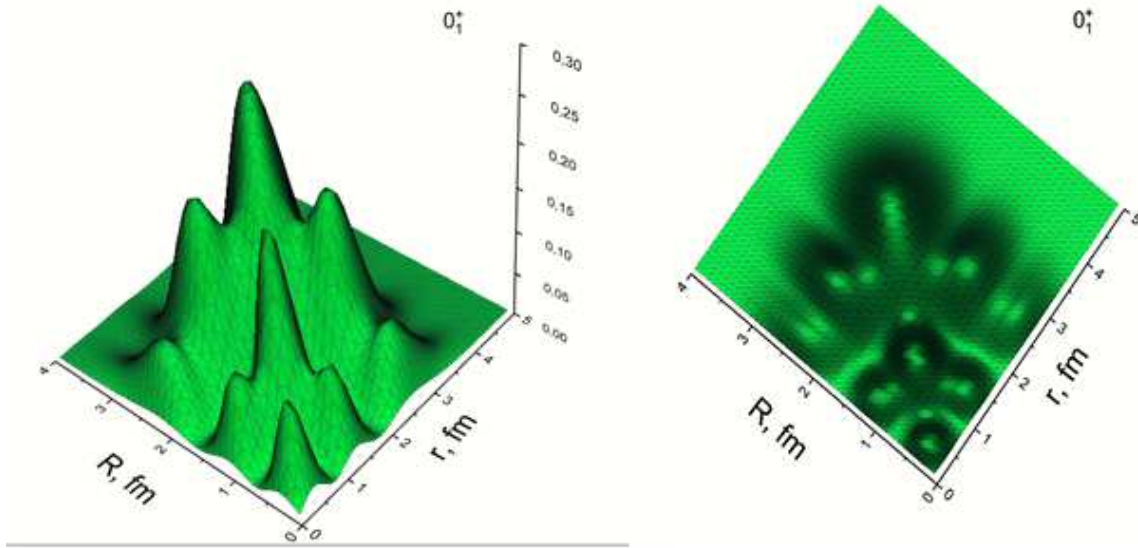


FIG. 1: Probability density for the  $^{12}\text{C}(0_1^+)$  ground state.

In Fig. 1 we show the probability density functions for the  $^{12}\text{C}(0_1^+)$  ground state. As can be seen from the figure, in this state the alpha particles mostly move in a regular triangular configuration with a maximum probability at the distance of  $r = 2.7$  fm and  $R = 2.5$  fm.

In Fig. 2 the probability density function for the  $^{12}\text{C}(0_2^+)$  Hoyle state is presented. Here one can see a very different structure of the matter distribution. In this state the two alpha particles move at the distance of about  $r = 4$  fm, and the last alpha particle moves far from the doublet at the distance between  $R = 3.0$  fm and  $R = 5.0$  fm. There is also a probability to go to smaller distances which corresponds to the smaller maxima in the structure function. Here both linear and  $^8\text{Be} + \alpha$  configurations are possible as was found in [16].

In Fig. 3 the probability density function for the  $^{12}\text{C}(2_1^+)$  bound state is demonstrated.

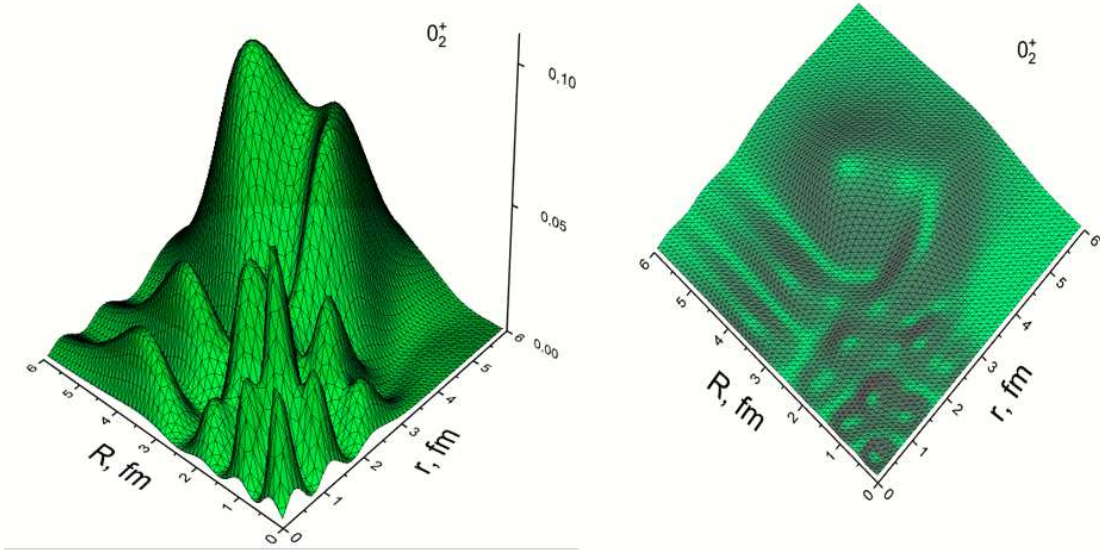


FIG. 2: Probability density for the  $^{12}\text{C}(0_2^+)$  Hoyle resonance state.

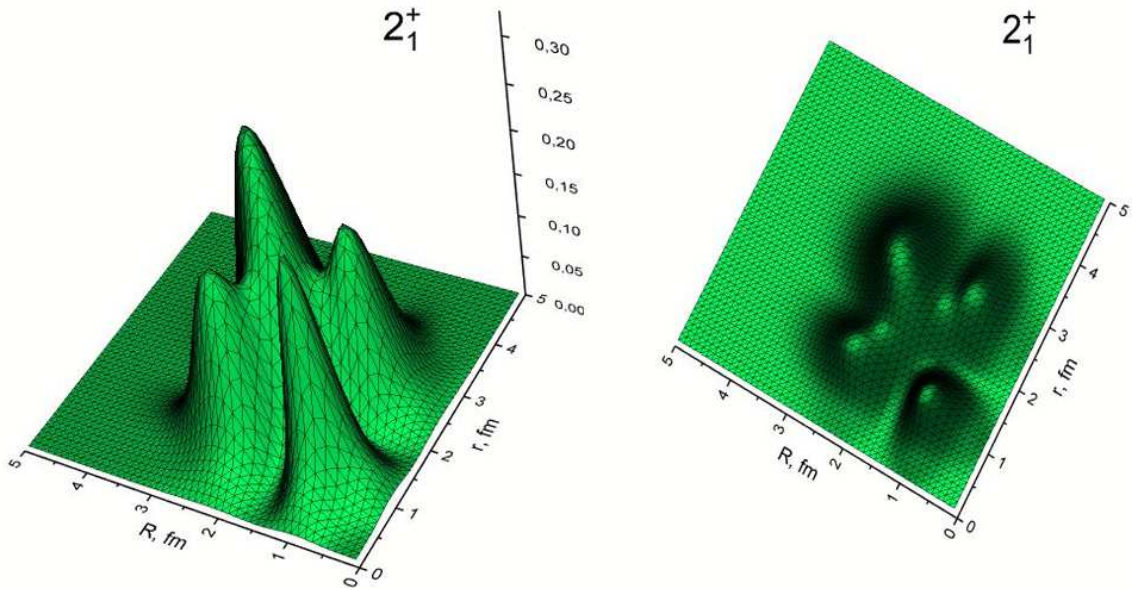


FIG. 3: Probability density for the  $^{12}\text{C}(2_1^+)$  excited bound state.

As can be seen from the figure, the spatial structure of this state is also triangular. It is close to the matter distribution of the ground state, but there is a difference at small distances.

In Fig. 4 the probability density function for the  $^{12}\text{C}(2_2^+)$  Hoyle analog state is presented. Here one can see a very extended structure. In this state the two alpha particles move at

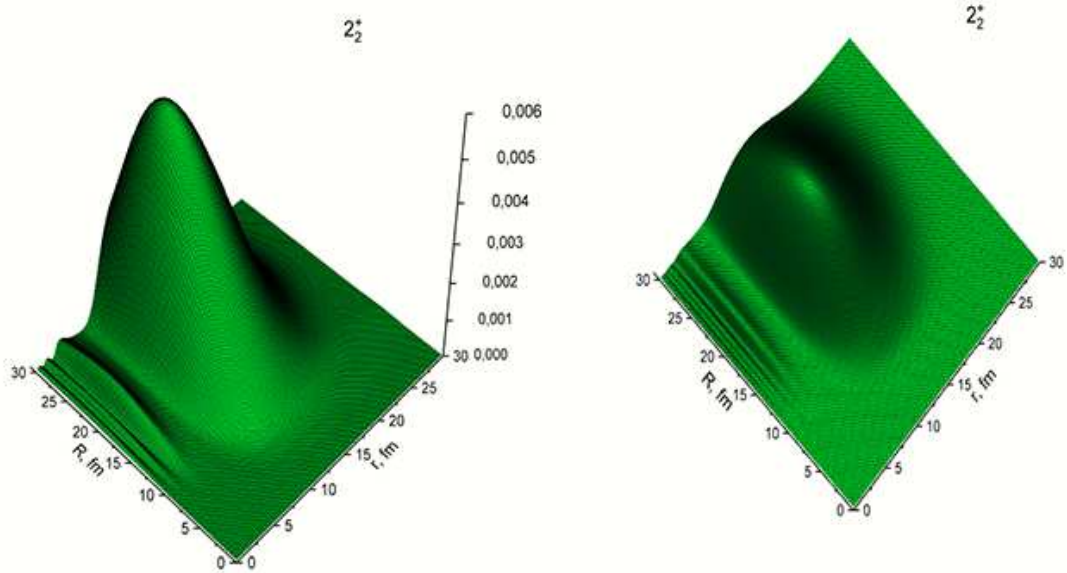


FIG. 4: Probability density for the  $^{12}\text{C}(2_2^+)$  Hoyle resonance analog state.

the distance about  $r = 15$  fm, and the last alpha particle moves far from the doublet at the distance between  $R = 15.0$  fm and  $R = 30.0$  fm.

#### IV. CONCLUSION

In summary, the spatial structure of the lowest  $0^+$  and  $2^+$  states of the  $^{12}\text{C}$  nucleus has been analyzed within the  $3\alpha$  model with the BFW  $\alpha\alpha$  potential with two forbidden states in the  $S$  wave and a single forbidden state in the  $D$  wave. The Pauli forbidden states in the three-body system were treated by the exact orthogonalization method. As was found previously, the ground and excited  $2_1^+$  bound states in the deep phases are completely defined by the so-called quantum critical eigen states of the three-body Pauli projector for the  $0^+$  and  $2^+$  functional spaces, respectively. In the weak phases these states are very close to the Hoyle and its analog states.

The contributions of different partial waves into the  $0_1^+$ ,  $0_2^+$ ,  $2_1^+$  and  $2_2^+$  states have been

estimated. For the ground and excited  $2_1^+$  bound states in the deep phases the largest contributions come from the partial waves  $(\lambda, \ell) = (2, 2)$  and  $(\lambda, \ell) = (4, 4)$ . In contrast to the bound states, for the Hoyle resonance  $0_2^+$  and its analog state  $2_2^+$ , dominant contributions come from the  $(\lambda, \ell) = (0, 0)$  and  $(\lambda, \ell) = (2, 2)$  configurations, respectively.

The estimated probability density functions for the  $^{12}\text{C}(0_1^+)$  ground and  $2_1^+$  excited bound states show mostly a triangular structure with a distance of about 2.5 fm between the  $\alpha$  particles. However, the spatial structures of the Hoyle resonance and its analog have a strongly different structure, like  $^8\text{Be} + \alpha$ . In the Hoyle state the last  $\alpha$  particle moves far from the doublet at the distance between  $R = 3.0$  fm and  $R = 5.0$  fm. Even more, in the Hoyle analog state the two alpha particles move at the distance of about 15 fm and the last  $\alpha$  particle goes far from the doublet at the distance between  $R = 15.0$  fm and  $R = 30.0$  fm.

- 
- [1] S. Elhatisari, N. Li, A. Rokash, et al., Phys. Rev. Lett. **117**, 132501 (2016).
  - [2] M. Freer, H. Horiuchi, Y. Kanada-Enyo, Dean Lee, and Ulf-G. Meissner, Rev. Mod. Phys. **90**, 035004 (2018).
  - [3] A. Tohsaki, H. Horiuchi, P. Schuck, and G. Röpke, Rev. Mod. Phys. **89**, 011002 (2017).
  - [4] Y. Suzuki, H. Matsumura, M. Orabi, Y. Fujiwara, P. Descouvemont, D. Baye, and M. Theeten, Phys. Lett. B **659**, 160 (2008).
  - [5] E. M. Tursunov, D. Baye, and P. Descouvemont, Nucl. Phys. A **723**, 365 (2003).
  - [6] B. Buck, H. Friedrich, and C. Wheatley, Nucl. Phys. A **275**, 246 (1977).
  - [7] V. I. Kukulin and V. N. Pomerantsev, Ann. Phys. (N.Y.) **111**, 330 (1978).
  - [8] E. M. Tursunov, D. Baye, and P. Descouvemont, Phys. Rev. C **73**, 014303 (2006).
  - [9] E. M. Tursunov, D. Baye and P. Descouvemont, Phys. Rev. C **74**, 069904 (2006).
  - [10] E. M. Tursunov, A. S. Kadyrov, S. A. Turakulov, and I. Bray, Phys. Rev. C **94**, 015801 (2016).
  - [11] D. Baye, and E. M. Tursunov, J. Phys. G: Nucl. Part. Phys. **45**, 085102 (2018).
  - [12] E. M. Tursunov, S. A. Turakulov, A. S. Kadyrov, and I. Bray, Phys. Rev. C **98**, 055803 (2018).
  - [13] H. Matsumura, M. Orabi, Y. Suzuki, and Y. Fujiwara, Nucl. Phys. A **776**, 1 (2006).
  - [14] E. M. Tursunov, J. Phys. G: Nuc. Part. Phys. **27**, 1381 (2001).
  - [15] E. M. Tursunov, and I. Mazumdar, Phys. At. Nucl. **85**, 160 (2021).
  - [16] V. V. Samarin, Eur. Phys. J. A **58**, 117 (2022).

- [17] E. M. Tursunov, Kh. D. Razikov, V. I. Kukulín, et al., *Phys. At. Nucl.* **57**, 2075 (1994).
- [18] E. M. Tursunov, *Pramana - J. Phys.* **95.**, 128 (2021).